Eur. Phys. J. D **12**, 153–159 (2000)

THE EUROPEAN PHYSICAL JOURNAL D

EDP Sciences

Buffer-gas effect on the rotovibrational line intensity distribution: Analysis of possible mechanisms

A.P. Kouzov[a], K.G. Tokhadze, and S.S. Utkina

Institute of Physics, Saint Petersburg State University, Peterhof, Saint Petersburg 198904, Russia

Received 17 January 2000

Abstract. Line intensities A_m ($|m| \leq 4$) of the HF fundamental band ($T = 293$ K) are found to decrease linearly with the buffer-gas (Xe) density ($d_{\rm Xe} = 2.6$–16 Amagat). The obtained slopes $\Delta_1(m)$ of the $A_m(d)/A_m(0)$ *vs.* $d_{\rm Xe}$ plots are maximum at $|m| = 1$ ($\Delta_1(1) \approx \Delta_1(-1) = 1.7(4) \times 10^{-2}$ Amagat^{-1}) and rapidly drop with $|m|$. Many possible mechanisms are considered; the most effective one appears to be the HF–Xe bimer formation, with the equilibrium constant strongly depending on the rotational quantum number. The rigid-rotator approximation used gives the density derivatives considerably smaller than the measured ones. The disbalance may be lessened for vibrating rotators by allowance for the interband intensity transfer induced by the vibrational modulation of short-range forces.

PACS. 33.20.Ea Infrared spectra – 33.70.-w Intensities and shapes of molecular spectral lines and bands – 34.10.+x General theories and models of atomic and molecular collisions and interactions (including statistical theories, transition state, stochastic and trajectory models, etc.)

1 Introduction

Despite the first evidences on the ability of buffer gases to selectively modify the line intensities within a vibrational band appeared in the sixties [1], the effect remains still poorly explored from both experimental and theoretical standpoints. To the best of our knowledge, the only extensive study performed so far is due to Piollet-Mariel, Boulet and Levy [2] who found the linear decrease of the integrated line intensities $A_{\rm IF}$ in the HCl overtone band on the buffer-gas (Ar, Xe) number density $d_{\rm b}$:

$$A_{\rm IF}(d_{\rm b})/A_{\rm IF}(0) \approx 1 + d_{\rm b}\Delta_{\Delta v}(m). \qquad (1)$$

The density coefficients $\Delta_2(m)$ ($m = \pm 1, \pm 2...$ is the line number) were all found to be negative, the strongest decrease ($\Delta_2(1) \approx -0.02$/Amagat) being observed for the $R_2(0)$-transition ($v_{\rm i} = 0, J_{\rm i} = 0) = I \rightarrow F = (v_{\rm f} = 2, J_{\rm f} = 1$). The measured $\Delta_2(m)$ rapidly disappear at higher rotational states. A similar J-dependence was found for the symmetric $P_2(J+1)$-lines.

The interpretation advanced in [2] was based on the static approach [3,4]:

$$A_{\rm IF} = \overline{\langle I'|\rho|I'\rangle\langle I'|\mathbf{M}|F'\rangle^2} \qquad (2)$$

that implies the lifetime $\tau_{\rm c}$ of intermolecular interactions to be infinitely long. The primed states corresponding to I and F collect all static perturbations; the upper bar denotes averaging over the interaction configurations. In so doing, the perturbation of the density matrix ρ was neglected, and only variations of the dipole moment matrix element $\langle I'|\mathbf{M}|F'\rangle$ were accounted for.

In our opinion, there are serious objections to this interpretation. First, the static theory cannot produce Lorentzian shapes, in apparent conflict with a wealth of observations including those of reference [2]. The non-Lorentzian static shapes may appear only at large detuning $\Delta\omega_{\rm FI}$ from the line centers when $\Delta\omega_{\rm FI}\tau_{\rm c} \gg 1$. Based on the known HCl–Ar potential [5], $\tau_{\rm c}^{-1}$ is estimated to be $\sim$ 20 cm^{-1} at room temperature. On the other hand, $\Delta\omega_{\rm FI}$ cannot exceed the half interval between the nearest lines equal to the rotational constant B. Thus, $\Delta\omega_{\rm FI}\tau_{\rm c} \leq B\tau_{\rm c} \approx 0.5$ showing the static picture to be improper.

Second, the demonstration of the linear density dependence in the static approach meets serious problems since the pairwise effect takes place only in the first perturbation order. The theory [2] is based rather on a postulate than on the hierarchy of physical times. On the contrary, the pairwise additivity in the dynamic approach is due to the inequality $\tau_{\rm c} \ll \tau_0$ (τ_0 is the mean time between successive collisions) which holds at the densities studied.

Third, the band integrated intensity $A_{\rm band} = \sum_m A_{\rm IF}$ can be strictly shown to be $d_{\rm b}$-independent for any rototranslational dynamics [6] provided:

(a) the collision-induced polarization is negligible,
(b) the local-field effects are disregarded,
(c) the vibration remains unperturbed by collisions,
(d) the bound-states contributions are negligible.

[a] e-mail: alex@apk.usr.pu.ru

The assumptions (b–d) were used in [2]; in addition, the incremental collision-induced absorption (a) was shown to be quite weak [2]. The appearing artifact total band-intensity dependence on density is because of the wave-function perturbations, by assumption, did not influence the matrix elements of ρ. With the provisos (a–d), a more consistent treatment incorporating all effects of perturbation should result in a sign-changing dependence $\Delta_0(m)$ not confirmed experimentally [2].

These contradictions led us to reexamine the problem from the more realistic dynamic (impact) standpoint. The results are presented in Section 3, where two points are emphasized. First, the rotational population redistribution is important, being mainly due to the bimer formation. Notice that the interaction potentials are substantially anisotropic (to mix the rotational states) and their well depths are close to kT (to populate the bound states). Second, the H–X stretching modes are characterized by large amplitudes comparable with the repulsion core length. At least in this range, vibration appreciably modulates the interaction and, as the result, the density matrix acquires off-diagonal vibrational elements. In the binary-collision regime, this leads to intensity mixing of different vibrational bands linear in d_b. In its turn, a considerable part of this vibrational intensity transfer may be attributed to bimers and thus should be J-dependent.

In the HF–Xe case, the bimer band was traced in our recent IR studies [7]. It is formed near the vibrational frequency and is well resolved from the neighbouring P- and R-lines at moderate pressures. Presently, we report the density behaviour of these lines associated with the unbound HF molecules. As compared to the HCl case, the line spacings are almost doubled amounting to about 40 cm^{-1} (B_HF = 20.56 cm^{-1}) that favours the intensity measurements.

2 Experimental results

The absorption spectra of the gaseous HF/Xe mixtures were recorded in the spectral range 3500–4200 cm^{-1} at relatively low Xe densities varied from 2.6 up to 16 Amagat. In this density range, the line overlap remains negligible, and accurate line-intensity measurements are possible. To measure A_IF with sufficient accuracy, the profiles were recorded at frequency detunings of five halfwidths to each side from the line center. The resulting uncertainty of the integrated line intensity did not exceed 0.5%. Since the broadening coefficients are typically of the order 0.1 cm^{-1}/Amagat, one can infer that the routine remains quite reliable for HF at the above densities, with the relative intensity variations reaching 10% or more.

The measurements were performed at T = 293 K using a stainless steel optical cell of the 10 cm pathlength with the leicosaphire windows. The density was calculated from the reference thermodynamic data [8]. The resolution of the Bruker 113v Fourier spectrometer used was 0.1 cm^{-1} to obtain the low-density spectra (d_b = 2.6–6 Amagat) and 0.2 cm^{-1} to record the line shapes at d_b = 6–16 Amagat.

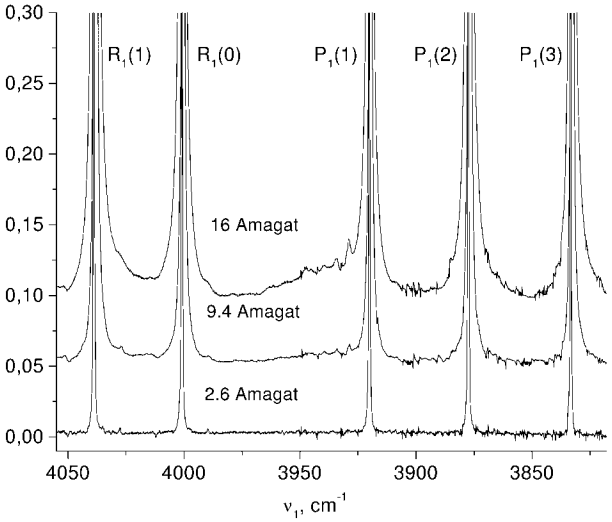

Fig. 1. Absorption spectra of HF–Xe mixtures (T = 293 K) at different Xe densities; the upper curves are vertically shifted by 0.05 and 0.10.

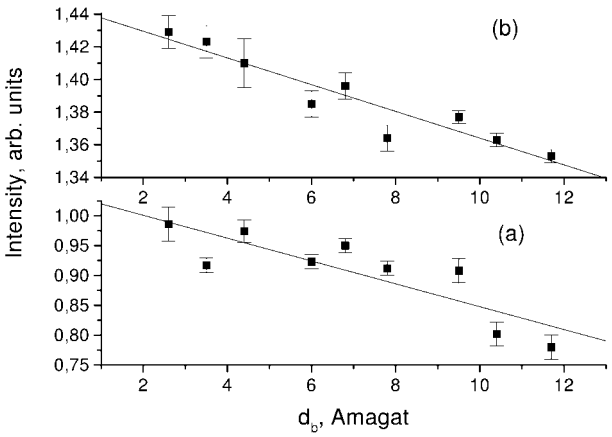

Fig. 2. Density dependence of HF line intensities on Xe density (T = 293 K): (a) R$_1$(0) transition; (b) R$_1$(1) transition.

The spectrum evolution on the Xe density is portrayed in Figure 1. At low density (d_b = 2.6 Amagat), the HF lines are characterized by the J-dependent halfwidths (0.2–0.7 cm^{-1}). As the Xe density grows, the lines are linearly broadened, and a new asymmetric band is steadily formed near the $P(1)$-line (Fig. 1). Based on its position and characteristic shape with the high-frequency shoulder, this band was assigned [7] to the HF stretching mode of the HF–Xe bimer. As noted in the high-density experiments [7], the lines with $|m| = 1, 2, 3$ became less intense with the growing Xe density, similarly to what was observed in the HCl–Ar/Xe spectra [2]. All spectra measured at different densities were normalized for the constant HF density assuming the total integrated intensity of the $R(3)$–$R(7)$ lines to be not subjected to d_b. Typical A_m *vs.* d_b plots are drawn in Figure 2. Table 1 lists values of the $\Delta_1(m)$ coefficients derived by the linear regression fits. Systematic deviations that could be assigned to the terms quadratic in d_b were not detected in the

Table 1. Negative density coefficients $\Delta_1(m)$ (in 10^{-2}/Amagat) for vibrotational line intensities of HF–Xe mixture.

	Measurement		Calculation for $R_0(J)/P_0(J+1)$ lines		
J	$R_1(J)$	$P_1(J+1)$	Bimer term	Bimer term	Quantum correction
	$T = 293$ K	$T = 293$ K	$T = 293$ K	$T = 200$ K	$T = 293$ K
0	1.9(4)	1.5(4)	0.225	0.473	0.47×10^{-2}
1	0.53(7)	0.8(1)	0.097	0.231	0.24×10^{-2}
2	0.22(7)	0.6(2)	0.023	0.066	-0.11×10^{-2}
3	0	0.3(3)	0.001	0.003	-0.88×10^{-2}
4	0	0	0	0	-1.52×10^{-2}

pressure range studied. A pair of central lines ($|m| = 1$) was found to have the largest Δ_1-values ($\Delta_1(1) \approx \Delta_1(-1) \approx -1.7(4)\times10^{-2}$ Amagat^{-1}). One may state that within the measuremental errors the $P_1(J+1)$- and $R_1(J)$-lines ($J = 0, 1$) have the same Δ_1-coefficients; the $P_1(3)$-line decrease is faster than that of the $R_1(2)$-line (Tab. 1). Such asymmetry in the HCl spectra [2] is seemingly absent. The effect might be attributed to the vibration-rotation interaction which is stronger in the HF case; however, a detailed consideration of $VR-T$ coupling remains beyond the scope of this study.

3 Analysis of possible contributions

To reveal the possible mechanisms of the density effect, we write the band spectral function $\Phi_{vv'}(\omega)$ as

$$\Phi_{vv'}(\omega) = \sum_{kk'} \int_{-\infty}^{\infty} \langle vk|\rho M(0)|k'v'\rangle \times \langle v'k'|M(t)|kv\rangle \exp(-\mathrm{i}\omega t)\mathrm{d}t \quad (3)$$

where k symbolizes the set of quantum numbers characterizing the rototranslational motion. The active molecule remains most of the time unperturbed; the second factor in the integrand (Eq. (3)) is then oscillating with the frequency ω_{FI} belonging to the specified $v \to v'$ band. Due to correlations imposed by the intermolecular interactions, the integrated band intensity becomes proportional to $\langle v|\rho M|v'\rangle\langle v'|M|v\rangle$ but not to $\langle v|\rho|v\rangle\langle v|M|v'\rangle^2$ as equation (2) implies. The difference between both expressions is due to the off-diagonal vibrational elements of ρ which are obviously density dependent since they disappear in a collisionless gas. Note also that the diagonal vibrational matrix elements of M are usually much larger than the off-diagonal ones. Hence, the effect of the off-diagonal $\langle v|\rho|v'\rangle$ elements on the pure rotational band (*i.e.* at $v = v' = 0$) is reduced. On the contrary, the nondiagonality of ρ may add much to the vibrational transition intensities since the intensity can be transfered from more intense bands with smaller values of Δv. Here, the calculations of the density effects are performed assuming $\langle v|\rho|v'\rangle = \delta_{vv'}\langle v|\rho|v\rangle$ to hold; such treatment is, strictly speaking, appropriate to the pure rotational band. In such case, the vibrational dependence of the intermolecular potential affects slightly, if any, the result. Arguments will be given for the possible vibrational interband intensity transfer. Apart from difficulties encountered in its calculation, the data are lacking on the off-diagonal vibrational elements of the potential which produce a nonvanishing value of $\langle v|\rho|v'\rangle$.

3.1 Reduced density matrix

We shall exploit the dynamical approach [9] based on the Fano theory [10]. The approach uses the symmetric Liouville-space metric [9], implying that the symmetrized band shape function $U(\omega)$ is first calculated and, with its help, the observable asymmetric band profile $\Phi(\omega)$ is then obtained. Provided the vibrational effects on the band shapes are negligible, such scheme exactly accounts for the detailed-balance. The integrated line intensities $\widetilde{A}_{\mathrm{IF}}$ in the $U(\omega)$-spectrum are [9]

$$\widetilde{A}_{\mathrm{IF}} = \langle v_{\mathrm{i}}J_{\mathrm{i}}|\mathbf{M}|J_{\mathrm{f}}v_{\mathrm{f}}\rangle^2\big[\langle J_{\mathrm{i}}|\widetilde{\rho}_a|J_{\mathrm{i}}\rangle + \langle J_{\mathrm{f}}|\widetilde{\rho}_a|J_{\mathrm{f}}\rangle\big]/2. \quad (4)$$

Instead of the conventially exploited free-molecule density matrix ρ_a [2,10], equation (4) contains the reduced density matrix $\widetilde{\rho}_a = \mathrm{Tr}_B\rho$; the trace is to be taken over the unbound bath (B) states. When $\mathbf{M}$ is assumed to be the dipole moment of a free molecule, the pressure effects are due to the difference between $\widetilde{\rho}_a$ and ρ_a: $\langle J|\widetilde{\rho}_a|J\rangle = \langle J|\rho_a|J\rangle[1 + d_{\mathrm{b}}F(J)]$. The correction to the measured line intensity A_{IF} (in the Φ-spectrum) is then reduced to

$$\Delta_0(m) = \frac{1}{1+\exp(-\beta\hbar\omega_{\mathrm{fi}})}\big[F(J_{\mathrm{i}}) + \exp(-\beta\hbar\omega_{\mathrm{fi}})F(J_{\mathrm{f}})\big]. \quad (5)$$

Obviously, the intensity corrections for the $P(J+1)$ and $R(J)$ lines coincide and, therefore, the rotational detailed balance equation: $A_{\mathrm{IF}}(J_{\mathrm{i}}, J_{\mathrm{f}}) = A_{\mathrm{IF}}(J_{\mathrm{f}}, J_{\mathrm{i}})\exp(h\omega_{\mathrm{fi}}/kT)$ holds.

Two independent mechanisms caused by binary intermolecular interactions can contribute to the density F-coefficients. The first one is due to the quantum rototranslational dynamics of colliding a–b pairs. The second mechanism originates from the a–b bimer formation that decreases the line intensities of the unbound molecules a. As will be shown below, the bimer-monomer equilibrium constant strongly depends on J, and therefore the intensity is selectively transfered from the rotational lines to the bimer band resulting in equation (1).

3.1.1 Quantum corrections

Except very low temperatures, the translational motion is classical. Neglecting the contribution from the bound trajectories, one can readily take the integrals over the translational velocity components. The quantum corrections to $\langle J|\widetilde{\rho}_a|J\rangle$ are caused by the noncommutativity of the rotational kinetic energy operator K and the anisotropic intermolecular interaction W. Such quantum rotational effects are the more pronounced, the higher is B: *a priori*, they cannot be neglected for hydrogen halides possessing the large rotational constants. Since the total band intensity under the conditions (b–d) is conserved, the quantum correction must be a sign-changing function of J.

For simplicity, we assume the anisotropic part of W to be smaller than $\beta^{-1} = kT$. Using the definition of the S-operator

$$\exp(-\beta H) \equiv \exp(-\beta K)S(\beta)\exp(-\beta W); \quad H = W + K \tag{6}$$

the assumption allows the expansion in powers of βW: $S = \sum_n S_n$, where $S_n \sim (\beta W)^n$. Starting with $S_0 = 1$, the series is generated by the iterative solution of the equation $\partial S/\partial\beta = -\exp(\beta K)W\exp(-\beta K)S + SW$ which is easily derived from equation (6). One then finds

$$S_1(\beta) = \beta W - \int_0^\beta \exp(\beta' K)W\exp(-\beta' K)\mathrm{d}\beta' \tag{7}$$

$$\langle J_1 m_1|S_1|J_2 m_2\rangle = \beta C(x)\langle J_1 m_1|W|J_2 m_2\rangle \tag{8}$$

where $x = \hbar\beta\omega_{J_1J_2}$, $C(x) = 1 - [\exp(x) - 1]/x$. The S_1-matrix is entirely off-diagonal because of $C(0) = 0$.

To preserve the hermiticity of $\exp(-\beta H)$, we write

$$\begin{aligned}\exp(-\beta H) &= \exp(-\beta H/2)\exp(-\beta H/2) = \\ &\exp(-\beta K/2)S(\beta/2)\exp(-\beta W)S^\dagger(\beta/2)\exp(-\beta K/2) \\ &\approx \exp(-\beta K/2)\exp(-\beta W)\exp(-\beta K/2) \\ &+ \exp(-\beta K/2)[S_1(\beta/2)\exp(-\beta W) \\ &+ \exp(-\beta W)S_1^\dagger(\beta/2)]\exp(-\beta K/2).\end{aligned} \tag{9}$$

Being bath-averaged, the first term of equation (9) gives $\rho_a(J)$. The correction due to S_1 is pairwise additive, and each interaction may be treated separately. We may thus substitute the total interaction energy by its particular term W and multiply the final result by the number of perturbers. Expand W and the exponent in the Legendre polynomials P_L: $W = \sum_L P_L(\lambda)W_L(R)$; $\exp(-\beta W) = \sum_L P_L(z)G_L(R)$, where λ is the cosine of the angle between $\mathbf{R}$ and the unit vector $\mathbf{n}_a$ along the molecular axis. In the first order, a straightforward calculation gives

$$\begin{aligned}F_q^{(1)}(J) &= 4\pi n_L R_m^3 \textstyle\sum_L I_L[\Phi_L(J) - \overline{\Phi_L}] \\ \Phi_L(J) &= \frac{2}{2J+1}\textstyle\sum_{J'}\langle J \parallel C^{(L)} \parallel J'\rangle^2\varphi(\beta\omega_{JJ'}/2)\end{aligned} \tag{10}$$

where n_L is the Loschmidt number,

$$\varphi(x) = 1 - \mathrm{sh}(x)/x; \quad \overline{\Phi_L} = \sum_J (2J+1)\rho_a(J)\Phi_L(J),$$

and $\langle J \parallel C^{(L)} \parallel J'\rangle$ is the reduced rotational matrix element of the spherical harmonics $C_m^{(L)}$ normalized to $\sqrt{4\pi/(2L+1)}$. The appropriate interaction length R_m (say, equal to the Lennard-Jones diameter) is introduced to make the radial integrals I_L

$$I_L = \frac{\beta R_m^{-3}}{2L+1}\int G_L(R)W_L(R)R^2\mathrm{d}R \tag{11}$$

dimensionless. Since $\varphi(0) = 0$, the isotropic part of the potential, which is diagonal in J, cannot change the intensity distribution. The integrals I_L were evaluated for the M5 potential [11] of HF–Xe. Qualitatively, the quantum effects due to the $R - T$ coupling are similar to the effective translational temperature rise occurring in the quasiclassical Maxwellian distribution [12]. Although the trend of $\Delta_0^{(q,1)}(J)$ is correct, its values are more than 2 orders less than the observed ones (Tab. 1). Such significant disagreement can hardly be attributed to the neglect of terms nonlinear in the interaction potential or to the inaccuracy of the M5 model.

3.1.2 Effects of bimer formation

So far we tacitly included all rotation-translation states, the free and bound ones, in the calculation. To derive the nonpositive bimer correction $F^{(\mathrm{b})}(J)$, we separate the unbound part $\widetilde{\rho}_a^{(\mathrm{f})}$ of $\widetilde{\rho}_a = \widetilde{\rho}_a^{(\mathrm{b})} + \widetilde{\rho}_a^{(\mathrm{f})}$

$$\begin{aligned}(2J+1)^{-1/2}\langle J \parallel \widetilde{\rho}_a^{(\mathrm{f})} \parallel J\rangle &= \\ (2J+1)^{-1}\sum_M \langle JM|\widetilde{\rho}_a - \widetilde{\rho}_a^{(\mathrm{b})}|JM\rangle &\\ \equiv \rho_0(J)[1 + F^{(\mathrm{b})}(J)d_\mathrm{b}].&\end{aligned} \tag{12}$$

In so doing, we shall exploit the classical dynamics for all degrees of freedom: this makes $\langle JM|\widetilde{\rho}_a|JM\rangle$ indiscernible from $\rho_0(J)$, which was used in equation (12). In the final formulas, we shall return to discrete values of J. Classically, the ratio of two rotational matrix elements in the rhs of equation (12) is given by

$$F^{(\mathrm{b})}(J)d_\mathrm{b} = -N\int_B \exp(-\beta H)\mathrm{d}\Gamma' \Big/ \int_T \exp(-\beta H)\mathrm{d}\Gamma' \tag{13}$$

where N is the total number of perturbers; $\mathrm{d}\Gamma'$ is the elementary volume of the total two-particle phase space Γ divided by the angular momentum differential $\mathrm{d}J$. The symbol B (or T) means that bound (or all) trajectories in Γ' contribute to the relevant integral.

To explicitly express $\mathrm{d}\Gamma'$, we write first

$$\mathrm{d}\Gamma = \mathrm{d}P_{\theta_a}\mathrm{d}P_{\varphi_a}\mathrm{d}\theta_a\mathrm{d}\varphi_a\mathrm{d}\Gamma_\mathrm{TR},$$

where $\mathrm{d}\Gamma_\mathrm{TR}$ is the translational part of the elementary volume; $P_{\theta_a} = I\dot{\theta}_a$ and $P_{\varphi_a} = I\dot{\varphi}_a\sin^2\theta_a$ are the momenta conjugate to the molecular angular variables and

I is the molecular moment of inertia. Upon transition to new variables $J = \sqrt{P_{\theta_a}^2 + (P_{\varphi_a}/\sin\theta_a)^2}$, $\mu = J_z/J = P_{\varphi_a}/J\sin\theta_a$, where J_z is the momentum projection onto the laboratory Z-axis, one obtains

$$\int_B \exp(-\beta H)\mathrm{d}\Gamma' = J\int_{-1}^{1}(1-\mu^2)^{-1/2}\mathrm{d}\mu \times \int \exp(-\beta H)\mathrm{d}\Omega_a\mathrm{d}\Gamma_{\mathrm{TR}} \qquad (14)$$

$$\int_T \exp(-\beta H)\mathrm{d}\Gamma' = 4J\rho_0(J)\pi^2 V(2\pi m/\beta)^{3/2}$$

where m is the reduced mass of the colliding pair, $\mathrm{d}\Omega_a = \sin\theta_a\mathrm{d}\theta_a\mathrm{d}\varphi_a$, and V stands for the gas volume.

The translational subspace Γ_{TR} is spanned by the translational momentum $\mathbf{P}$ and the intermolecular separation $\mathbf{R}$ so that an exact 9D integration (Eq. (14)) meets difficulties; the main one is to decide whether the phase point $(J, \mu, \mathbf{n}_a, \mathbf{R}, \mathbf{P})$ belongs or does not to the bound trajectory. Strong coupling between the molecular rotation and the translational motion makes the whole task very much similar to the MD simulation.

Presently, we give only a lower bound estimation of $F^{(\mathrm{b})}(J)$ accounting for states with the negative total energy ($H < 0$). It neglects the contribution from the positive-energy domain where orbiting trajectories are possible (metastable quantum bimers). For atomic van-der-Waals bimers [13], the orbiting states increase the bimer/monomer equilibrium constant by 20–40% that roughly estimates from the above the accuracy of our calculation. Expectedly, the accuracy achieved is somewhat higher since orbiting is partially destroyed by RT-coupling. The latter is tacitly implied to be sufficiently strong. Were it not, the bimer intensity would be distributed over the whole band, and it would be difficult to separate it from the monomer intensity.

In the negative-energy domain, one can integrate over μ and three spherical angles of $\mathbf{R}$ and $\mathbf{n}_a$ to obtain $F^{(\mathrm{b})}(J) = -4\pi n_L R_m^3 f(\varepsilon_J)$, where the dimensionless function $f(\varepsilon_J)$

$$f(\varepsilon_J) = \pi^{-1/2}\iint_S \gamma(3/2, -(\varepsilon_J + \beta W)) \times \exp(-\beta W)\rho_m^2\mathrm{d}\rho_m\mathrm{d}\lambda \qquad (15)$$

depends on $\varepsilon_J = BJ(J+1)/kT$ rather than on J; $\gamma(n,x)$ is the incomplete gamma function, $\rho_m = R/R_m$. The integration area S is confined by $\varepsilon_J + \beta W \le 0$.

The higher is the rotational energy, the less probable is the bimer formation; moreover, the function $F^{(\mathrm{b})}(J)$ vanishes at the threshold value $J_{\max}$. Based on the M5 potential of HF–Xe [11], we found $J_{\max} = 4$. The function $-F^{(\mathrm{b})}(J)$ may be interpreted as the J-dependent constant of equilibrium between the free and bound active molecules; the population-weighted summation of $-nF^{(\mathrm{b})}(J)$ over J thus gives the total fraction of the bound HF molecules. Moreover, if one assumes the dipole moment of bimer to coincide with that of free molecule and disregards the vibrational effects, the band intensity $A_{vv'}$ becomes not subjected to the buffer-gas pressure: $A_{vv'} = A^{(\mathrm{f})}_{vv'} + A^{(\mathrm{b})}_{vv'} = \text{constant}$.

The calculated $\Delta_0^{(\mathrm{b})}(m)$ coefficients for HF–Xe are collected in Table 1. Apart of the J-threshold presence, the bimer contribution to Δ_0 rapidly grows with decreasing temperature (Tab. 1). The calculation reproduces the rapid decrease of $\Delta_0^{(\mathrm{b})}(m)$ at the rotational excitation, but the absolute values are approximately 6 times smaller than the measured ones. Moreover, similar calculations for HCl–Xe and HCl–Ar based on Hutson's potential [5] appeared to be in the same disbalance with the experiment [2]. Since the potentials used are known to describe well the rigid-rotator interactions with atoms [5], we are to conclude that there exist other mechanisms contributing to the density effects.

3.1.3 Line interference contributions

So far, we neglected the line mixing effect caused by the nonsecular part of the rotational relaxation matrix $\Gamma(\omega)$. To obtain the corrected spectrum function $S_m(\omega)$ of the mth line centered at ω_m, one should treat the off-diagonal Γ-matrix elements as a perturbation [14]. Along with the conventional Rosenkranz asymmetry term [14] (which has no effect on the integrated line intensity), we derived a new correction

$$\Delta_0^{(\mathrm{nd})}(m) = -\sum_{m'\neq m}[\Gamma'_{mm'}(\omega_m) + \Gamma'_{m'm}(\omega_{m'})] \times A_{m'}/A_m(\omega_m - \omega_{m'}) \qquad (16)$$

that appears due to the allowance for the imaginary terms $\Gamma'_{mm'}$ of Γ neglected by Rosenkranz [14].

This mechanism conserves the total band intensity, *i.e.* $\sum_m \Delta A_m = \sum_m \Delta_0^{(\mathrm{nd})}(m)A_m^2 = 0$ since the antisymmetric function of m and m' is summed. To the best of our knowledge, no model has been so far developed for the imaginary part of the rotational Γ-matrix. For a rough estimation, assuming $\Gamma'_{mm'}$ in equation (16) to be of constant sign, one can apply the sum rules [15] to obtain $|\Delta_0^{(\mathrm{nd})}(m)| < |\Gamma'_{mm}(\omega_m)|/B$. The measured rotational shift coefficients are typically 10^{-3} cm^{-1} Amagat^{-1} [16]; therefore, the line interference effect in the HF spectra is $\sim 10^{-4}$ Amagat^{-1} and cannot noticeably change the line intensities.

3.2 Influence of vibration

The inclusion of vibration may become important. At first sight, this should not be the case: Hutson's data [5] show the expectation values of the potential parameters to vary by about 1% or less on the vibrational excitation. Note, however, that these variations are quadratic in the small parameter $\chi = \sqrt{2B/\hbar\omega_0}$ ($\chi_{\mathrm{HF}} = 0.10$) whereas the nonsecular vibrational terms of potential (and of the density matrix) are linear in χ.

In the impact theory, the interband correlation is caused by the nonorthogonality of the vibrational line-space vectors. (Within each band, nevertheless, the line-space orthogonality is preserved since the reduced density matrix remains isotropic and, consequently, diagonal.) The generalization of the line-space metric that incorporates the vibrational effects without violation of the rotational detailed balance is not trivial and shall not be discussed here. We just demonstrate that the vibrational intensity transfer is possible.

Consider the short-range part of the isotropic potential term $W_0(R)$ derived, say, from the atom-atom scheme. Due to the large mass difference, the heavier atom is placed practically at the center-of-mass whereas the H atom is shifted by $\mathbf{r}$ from it ($r \ll R$). Assuming the repulsion to be exponential with the core radius $\alpha^{-1}$and averaging over the orientations, one then obtains

$$W_0(R,x) \approx W_0(R,0)\exp(\alpha r_0 x)$$

where $x = r/r_0 - 1$ is the dimensionless vibrational displacement and r_0 stands for the equilibrium H–F distance. The above expression was derived having regard that for the systems considered $\alpha r_0 \approx 3$–4 holds [5,11]. It means that the repulsion interaction is strongly modulated by the H–F stretching. For the relevant matrix element, one has $\langle v|\exp(\alpha r_0 x)|v+\Delta v\rangle \sim (\alpha r_0\chi)^{|\Delta v|}$, where the dimensionless parameter $\alpha r_0\chi$ is comparable to unity. An order-of-magnitude estimation of the intensity transfer to the weaker $0 \to v+1$ band ($v \geq 0$) from the $0 \to v$ one results in the density coefficient $F_{v,v+1} \sim 4\pi R_m^3 n_L(\alpha r_0 kT/\hbar\omega_0)$ falling in the range 10^{-3}/Amagat. Therefore, the vibrational effects deserve a further theoretical study. We comment also, that the above estimation accounts neither for the anisotropic repulsion (which is vibration-dependent at the same extent), nor for the influence of the potential well; their allowance may considerably change the value of $F_{v,v+1}$.

The presence of the large-amplitude mode is seemingly essential for the intensity transfer: otherwise, the vibrational modulation of the interaction is weak. The Raman data on the vibrational intensity change per molecule at the gas-liquid transition collected by Schrötter and Klöckner [17] confirm this supposition: only the H(D)–X stretching bands in the halogenated methanes are enhanced by the density. It should also be noted that the role of the bound states in the vibrational intensity transfer can differ from that in the rigid rotator case. In particular, the ratio of the bimer/monomer intensities in the vibrational bands may not be given by the relevant equilibrium constant. Data on the pure rotational spectra (*e.g.*, the Raman ones) would be decisive to check the above hypothesis: the interband effect is expectedly negligible for them, with the density coefficients falling into the range of 10^{-3}/Amagat (Tab. 1).

3.3 Polarization effects

In this section we briefly examine the electrooptical effects that may alter the transition amplitudes (see Eq. (2)) due to the influence of medium. The effects may originate from variations of the electric-dipole coupling with the incident em field (the local-field effect) and from variations of the dipole moment itself (the reaction-field effect). However, the known local-field correction $\Delta^{(\mathrm{lf})}$ [18] is J-independent

$$\Delta^{(\mathrm{lf})} = 8\pi n_L \alpha_\mathrm{b}/3 \tag{17}$$

(α_b is the polarizability of the buffer particles) and appears to be of the incorrect sign and magnitude (1–2 decimal orders smaller than the experimental values). For the leading (isotropic) second-order reaction-field correction $\Delta^{(\mathrm{rf},2)}$, one has $\Delta^{(\mathrm{rf},2)} \sim \Delta^{(\mathrm{lf})}\alpha_a/R_m^3$ showing it to be negligible since α_a is 1–2 orders smaller than R_m^3. In accord with this estimation, the reaction-field approach to the band intensity variations caused by the gas-liquid transition (for the same mixtures as those considered here) resulted in the intractable values of the Onsager radius, two times smaller than the interaction diameter.

In contrast to $\Delta^{(\mathrm{lf})}$ and $\Delta^{(\mathrm{rf},2)}$, the first-order reaction-field correction $\Delta^{(\mathrm{rf},1)}$ may be, in principle, J-dependent, and we calculate it for a more complete picture. This correction is due to the dipole moment $\mu = \alpha_\mathrm{b}\mathbf{E}$ induced on the atom b by the electric dipole field $\mathbf{E}(\mathbf{M}_\mathrm{IF})$ of the particle a. The intensity variation is due to the in-phase part of μ_IF and is proportional to the mean scalar product doubled $2\langle(\mathbf{M}_\mathrm{IF},\mu_\mathrm{FI})\rangle$. The latter is nonzero only when the interaction potential W is anisotropic. Assuming the rototranslational motion to be semiclassical, we derived the expression

$$\Delta_{\Delta v}^{(\mathrm{rf},1)} = -\frac{16\pi n_L \alpha_\mathrm{b}}{25}\int_0^\infty G_2(R)R^{-1}\mathrm{d}R \tag{18}$$

which, in fact, appeared to be J-independent. The radial integration performed with the M5 potential of HF–Xe [11] gives $\Delta_{\Delta v}^{(\mathrm{rf},1)}/\Delta^{(\mathrm{lf})} = 0.02$. Thus the reaction-field contributions are too weak to explain the observations.

There is also an additional collision-induced absorption entirely due to μ_IF. Because of strong translational modulation, its lines are broad (about 30 cm^{-1}) and form a hardly detectable background. Moreover, the collision-induced correction as compared to $\Delta^{(\mathrm{lf})}$ contains an additional small factor α_b/R_m^3 (≈ 0.08 for HF–Xe) and is thus quite negligible. Previous calculations of this effect for HCl [2] led to similar results.

4 Conclusions

This study presents new data on the yet poorly studied selective line-intensity changes by buffer-gas pressure. The theoretical analysis undertaken was stimulated by apparent inconsistencies of the previously exploited static approach that accented only on the perturbations of the transition amplitudes. We found also that neither the in-phase polarization of buffer particles by the molecular dipole moment, nor the local-field effect can explain the observed J-dependent intensity variations. The magnitudes of these effects appear to be quite small; same holds

either for the quantum rotational corrections due to non-commutativity of the angular momentum with the interaction potential, or for rotational line mixing. In fact, only the bimer effect presently estimated for rigid molecules gives a correct order of the line intensity variations on density. For vibrating molecules, this effect can be enhanced by the interband intensity transfer due to the pronounced modulation of the interaction energy by the light-atom vibration. To appreciate the relative roles of the rotational and vibrational contributions, new IR and Raman measurements are desirable at different temperatures. This could provide new data on the vibration-dependent interaction surfaces and allow us to penetrate better into the nature of the intensity variations in more dense media.

Financial support of the Russian Foundation for Basic Research (Project Nos. 96-03-34097a and 97-03-33655a) is gratefully acknowledged.

References

1. M. Atwood, H. Vu, Compt. Rend. **264**, 1803 (1967).
2. E. Piollet-Mariel, C. Boulet, A. Levy, J. Chem. Phys. **74**, 900 (1981); *ibid.* **76**, 787 (1981).
3. D. Robert, M.R. Atwood, L. Galatry, C.R. Acad. Sci. (Paris) B **266**, 182 (1968).
4. R.M. Herman, J. Chem. Phys. **52**, 2040 (1970).
5. J.M. Hutson, J. Phys. Chem. **96**, 4237 (1992).
6. R.G. Gordon, J. Chem. Phys. **39**, 2788 (1963); *ibid.* **40**, 1973 (1964); *ibid.* **41**, 1819 (1964).
7. K.G. Tokhadze, S.S. Utkina, N.N. Filippov, Z. Milke, Opt. Spektrosk. **79**, 536 (1995).
8. *Handbook on the Thermophysical Properties of Gases and Liquids*, edited by N.B. Vargaftik (Nauka, Moscow, 1972).
9. A.P. Kouzov, J.V. Buldyreva, Chem. Phys. **221**, 103 (1997).
10. U. Fano, Phys. Rev. **131**, 259 (1963).
11. J.M. Hutson, B.J. Howard, Mol. Phys. **45**, 791 (1982).
12. L.D. Landau, Ye.M. Lifshitz, *Theoretical Physics* (Nauka, Moscow, 1976), Chap. 33, Vol. 5.
13. D.E. Stogryn, J.O. Hirschfelder, J. Chem. Phys. **31**, 1531 (1959).
14. P.W. Rosenkranz, IEEE Trans. Ant. Propag. **23**, 498 (1975).
15. M.O. Bulanin, A.B. Dokuchaev, M.V. Tonkov, N.N. Filippov, J. Quant. Spectrosc. Rad. Transfer **31**, 521 (1984).
16. I.M. Grigoriev, M.V. Tonkov, N.N. Filippov, Opt. Spectrosc. **77**, 185 (1994).
17. H.W. Schrötter, H.W. Klöckner, in *Raman Spectroscopy of Gases and Liquids*, edited by A. Weber (Springer Verlag, Berlin, 1979), Chap. 4.
18. M. Born, E. Wolf, *Principles of Optics* (Pergamon Press, Oxford, 1964).